COMBINED EFFECT OF IBS AND IMPEDANCE ON THE LONGITUDINAL BEAM DYNAMICS*

A. Blednykh[†], B. Bacha, G. Bassi, V. Smaluk, T. Shaftan

Brookhaven National Laboratory, Upton, NY, USA

M. Borland, R. Lindberg

Argonne National Laboratory, Argonne, IL, USA

Abstract

The horizontal/vertical emittances, the bunch length, and the energy spread increase have been studied in the NSLS-II as a function of a single bunch current. The monotonic growth of the horizontal emittance and the energy spread dependence on the single bunch current below the microwave instability threshold can be explained by the Intrabeam Scattering (IBS) effect. IBS results in an increase in the bunch length and the microwave instability thresholds. This was observed experimentally by varying the vertical emittance. To compare with experimental data, particle tracking simulations have been performed with the ELEGANT code including both IBS and the total longitudinal wakefield calculated from the 3D electromagnetic code GdfidL. The same particle tracking simulations have also been applied for the APS-U project, where IBS is predicted to produce only a marginal effect.

INTRODUCTION

The 3-GeV NSLS-II storage ring operates with a horizontal emittance $\varepsilon_x < 1$ nm rad [1, 2]. A set of measurements has been performed in NSLS-II to study the microwave instability threshold (I_{th}) behavior vs. single bunch current (I_0). A new microwave instability pattern was experimentally observed at $I_0 > I_{th}$ by measuring the energy spread dependence $\sigma_\delta(I_0)$ [3]. The experimental data agree well with particle tracking simulations performed with the SPACE [4] and ELEGANT [5] codes, which included the total longitudinal wakefield $W_\parallel(s)$ from numerical simulations with GdfidL [6] for a 0.3 mm bunch length [7]. All simulations were performed with fixed horizontal emittance $\varepsilon_x = 0.9$ nm, assuming that ε_x does not change at $I_0 > I_{th}$.

In this paper, we report on studies of the combined effect of IBS and impedance on the longitudinal beam dynamics below the microwave instability threshold, $I_0 < I_{th}$, specifically studying effects on the vertical and horizontal emittances $\varepsilon_{x,y}(I_0)$, bunch length $\sigma_\tau(I_0)$, and energy spread $\sigma_\delta(I_0)$.

IBS

The evidence of the IBS effect in NSLS-II on the energy spread increase at $I_0 < I_{th}$ has been observed experimentally [3] using a synchrotron light monitor (SLM). As shown in Fig. 1, the energy spread $\sigma_\delta(I_0)$ for different RF voltages growths monotonically with I_0 for $I_0 < I_{th}$ until the electron beam becomes longitudinally unstable, due to the total longitudinal impedance of the storage ring. In Fig. 2, we show the bunch length dependence $\sigma_\tau(I_0)$ measured by the streak camera at the RF voltage $V_{RF} = 3$ MV.
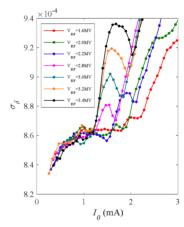

Figure 1: The energy spread σ_δ as a function of single-bunch current I_0 obtained from the SLM measurements of $\sigma_x(I_0)$ for the 3DW regular lattice.
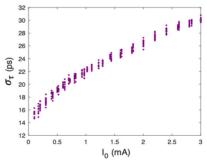

Figure 2: The measured bunch length as a function of single bunch current for the 3DW regular lattice at $V_{RF} = 3$ MV.

The energy spread growth below the microwave instability threshold is dominated by IBS. To show this, Figs. 3 and 4 compare predictions using several different
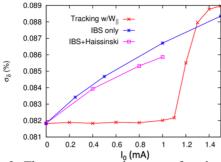
Figure 3: The energy spread σ_δ as a function of single-bunch current I_0 obtained by particle tracking simulations. The red trace includes the total wakefield only. The blue trace is the result estimated with the IBS effect only. Magenta trace includes IBS and bunch lengthening effect (Haissinski solution).
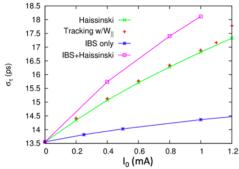

Figure 4: The bunch length as a function of single bunch current. The blue trace includes IBS only. The green trace represents the results of the numerical simulations using a Haissinski solver. The red crosses are tracking with the total longitudinal wakefield. The magenta trace is the combined effect of IBS and the Haissinski solution.

models. The red points plot particle tracking results using ELEGANT and the longitudinal impedance only, which shows no energy spread growth for $I_0 < I_{th}$, at which current the bunch lengthening is ~3.5 ps. This bunch lengthening is significantly larger than that predicted by the ibsEmittance [8] code, but the latter displays a noticeable energy spread increase that is consistent with the numerical observations made in Ref. [9]. The IBS calculation uses a 1% fixed emittance ratio. Predictions that include both IBS and wakefields are plotted with the magenta lines, which show somewhat less energy spread growth because the IBS effect is slightly mitigated by the bunch lengthening that is larger than that predicted from wakefields alone. We included both IBS and wakefields by using ibsEmittance to first obtain the energy spread, which is then used in the Hassinski solver [10] available with ELEGANT. The latter solves for the bunch length using the wakefield. Iterating between the two codes converges to the solution shown in magenta.

To simulate $\sigma_\delta(I_0)$ and $\sigma_\tau(I_0)$ below and above the microwave instability threshold properly, the IBS effect and the total longitudinal wakefield were included in ELEGANT for particle tracking simulations using the element-by-element NSLS-II lattice. The NSLS-II lattice

has 596 ZLONGIT elements and 1192 ZTRANSVERSE elements, the larger number of ZTRANSVERSE elements being explained by the need to separate elements for the dipole and quadrupole wakes. A single IBSCATTER element was inserted at the end of the lattice. It was set to use 30 longitudinal slices and used the smooth method of applying IBS effects, by virtue of which the particle amplitudes are uniformly increased according to the instantaneous growth rate. This is less noise-prone than using a more literal scattering algorithm.

The results of comprehensive ELEGANT simulations are compared with the experimental data in Figs. 5-9. After several beam studies and some efforts in tuning of the diagnostic tools, we were able to measure the horizontal $\varepsilon_x(I_0)$ and vertical emittance $\varepsilon_y(I_0)$ dependences from a non-dispersive source point using a pinhole camera for soft X-ray emission. The horizontal beam size $\sigma_x(I_0)$ and the bunch length $\sigma_\tau(I_0)$ dependence measured by the SLM camera and the streak camera respectively.
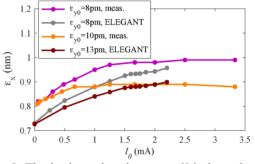

Figure 5: The horizontal emittance $\varepsilon_x(I_0)$ dependence at $V_{RF} = 3$ MV. The experimental and particle tracking data are for $\varepsilon_{y0} = 8$ pm and $\varepsilon_{y0} = 10$ pm lattices.
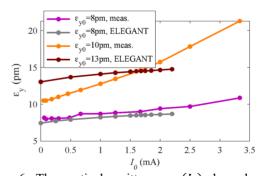

Figure 6: The vertical emittance $\varepsilon_y(I_0)$ dependence at $V_{RF} = 3$ MV. The experimental and particle tracking data collected for $\varepsilon_{y0} = 8$ pm and $\varepsilon_{y0} = 10$ pm lattices.

The simulations show monotonic horizontal emittance growth as function of single-bunch current, while the experimental data shows that ε_x saturates at I_0=1.5 mA for $\varepsilon_{y0} = 8$ pm and at I_0=0.6 mA for $\varepsilon_{y0} = 10$ pm. The simulations and the experimental data for $\varepsilon_y(I_0)$ dependence for $\varepsilon_{y0} = 8$ pm lattice agree well, while for $\varepsilon_{y0} = 10$ pm lattice the results diverge. This can be explained by the fact that we started the experiment with a
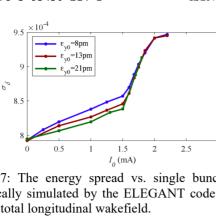
Figure 7: The energy spread vs. single bunch current numerically simulated by the ELEGANT code with IBS and the total longitudinal wakefield.
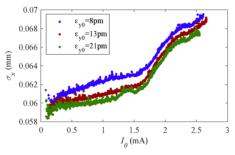

Figure 8: The experimental data of the horizontal beam size vs. single-bunch current measured by the SLM camera $\varepsilon_{y0} = 8$ pm, $\varepsilon_{y0} = 13$ pm and $\varepsilon_{y0} = 21$ pm lattices.
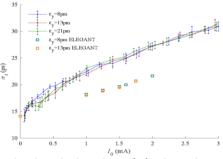

Figure 9: The bunch length $\sigma_\tau(I_0)$ dependence. The experimental data collected for $\varepsilon_{y0} = 8$ pm, $\varepsilon_{y0} = 13$ pm and $\varepsilon_{y0} = 21$ pm lattices.

well-optimized 8 pm lattice and, to increase the vertical emittance up to 10 pm, changed one quadrupole without further lattice optimization. This could introduce vertical dispersion, which could lead to a significant vertical emittance growth. The experiment will be repeated for a well-optimized 10 pm lattice to confirm the results. In Figs. 7 and 8 we plot the energy spread as a function of single bunch current simulated with ELEGANT and the horizontal beam size $\sigma_x(I_0)$ dependence measured by the SLM camera for three vertical emittances. As can be seen from these results, the IBS effect can help to suppress the microwave instability threshold. For higher vertical emittance, the IBS effect becomes weaker (the bunch length becomes shorter), and the microwave instability threshold gets smaller.

From Fig. 8 it follows that the experimentally obtained microwave instability threshold is $I_{th} = 1.2$ mA for a

$\varepsilon_{y0} = 21$ pm and $I_{th} = 1.6$ mA for a $\varepsilon_{y0} = 8$ pm. The particle tracking simulations (Fig. 7) confirm the experimental data.

The measured bunch length $\sigma_\tau(I_0)$ dependence by the streak camera for different emittances is plotted in Fig. 9. We were not able to identify any changes in bunch lengthening by varying the initial vertical emittance from $\varepsilon_{y0} = 8$ pm to $\varepsilon_{y0} = 21$ pm, probably due to the limited streak camera resolution. The IBS effect gives another 10% increase in bunch lengthening, in addition to the bunch lengthening due to the total longitudinal wakefield, but still the numerical results are different from the experimental data by a factor of 1.3.

CONCLUSION

We continue to investigate the difference in bunch lengthening between experiment and simulation. The present NSLS-II wakefield does not include the wakefields of five titanium-coated ceramic chambers. However, with the present total longitudinal wakefield we can reproduce the energy spread distribution below and above the microwave instability threshold, including the microwave fill-pattern [3].

It should be noted that the estimated horizontal emittance at low current is $\varepsilon_x(I_0 \to 0) = 0.74$ nm. We see ~10% increase of ε_x during operation in NSLS-II at $I_{av} = I_0 M = 500$ mA within $M = 1205$ bunches, which is in agreement with the numerical results of Ref. [11] performed by the ZAP code [12] for 820 MeV radiation losses. In the present work we extend our study above the NSLS-II required parameters and perform the particle tracking simulations for a wide range of parameters.

The single-bunch transverse coupled mode instability (TMCI) threshold in NSLS-II is $I_{th,TMCI} = 0.7$ mA at chromaticity $\xi_{x,y} = +2$. The vertical emittance growth does not change by running at higher positive chromaticity of +4 or with use of the transverse bunch-by-bunch feedback system up to $I_0 = 4$ mA.

REFERENCES

[1] G. M. Wang *et al.*, "Emittance and lifetime measurement with damping wigglers", *Rev. of Sci. Instrum.,* vol. 87, p. 033301, 2016. doi:10.1063/1.4942903

[2] V. Smaluk *et al.*, "Effect of undulators on magnet lattice and emittance", *Phys. Rev. Accel. Beams*, vol. 22, p. 124001, 2019. doi:10.1103/PhysRevAccelBeams.22.124001

[3] A. Blednykh *et al.*, "New aspects of longitudinal instabilities in electron storage rings", *Sci. Rep.*, vol. 8, p. 11918, 2018. doi:10.1038/s41598-018-30306-y

[4] G. Bassi, A. Blednykh, and V. Smaluk, "Self-consistent simulations and analysis of the coupled-bunch instability for arbitrary multibunch configurations", *Phys. Rev. Accel. Beams*, vol. 19, p. 024401, 2016. doi:10.1103/PhysRevAccelBeams.19.024401

[5] M. Borland, "ELEGANT: A Flexible SDDS-Compliant Code for Accelerator Simulation", ANL, Argonne, IL, USA, Rep. ANL/APS LS-287, Aug. 2000.

[6] W. Bruns, http://www.gdfidl.de

[7] A. Blednykh, G. Bassi, C. Hetzel, B. Kosciuk, and V. Smaluk, "NSLS-II longitudinal impedance budget", *Nucl. Instrum. Methods Phys. Res.*, vol. 1005, p. 165349, 2021. `doi:10.1016/j.nima.2021.165349`

[8] M. Borland, L. Emery, H. Shang, and R. Soliday, "SDDS-Based Software Tools for Accelerator Design", in *Proc. of the 2003 Bipolar/BiCMOS Circuits and Technology Meeting*, paper 03CH37440, pp. 3461-3463, 2003. `doi:10.1109/pac.2003.1289948`

[9] F. H. de Sá, "Collective Instability Studies for Sirius", in *Proc. IPAC'19*, Melbourne, Australia, May 2019, pp. 61-64. `doi:10.18429/JACoW-IPAC2019-MOPGW003`

[10] J. Haïssinski, "Exact longitudinal equilibrium distribution of stored electrons in the presence of self-fields", *Nuov. Cim. B*, vol. 18, pp. 72–82, 1973. `doi:10.1007/BF02832640`

[11] B. Podobedov and L. Yang, "IBS Effects in a Wiggler Dominated Light Source", in *Proc. 22nd Particle Accelerator Conf. (PAC'07)*, Albuquerque, NM, USA, Jun. 2007, paper TUPMS078, pp. 1353-1355.

[12] M. S. Zisman, S. Chattopadhyay, and J. J. Bisognano, "ZAP user's manual", Lawrence Berkeley Lab., CA, USA, Rep. LBL-21270; ESG-15, Dec. 1986.